ONIOM Studies of Chemical Reactions on Carbon Nanotube Tips: Effects of the Lower Theoretical Level and Mutual Orientation of the Reactants

Vladimir A. Basiuk*

Instituto de Ciencias Nucleares, Universidad Nacional Autónoma de México, Circuito Exterior C.U., A. Postal 70−543, 04510 México D.F., Mexico

Received: March 31, 2003; In Final Form: June 9, 2003

We studied theoretically the interaction of simple aliphatic amines with carboxylated zigzag and armchair single-walled carbon nanotube (SWNT) models. We used single-level MM+ molecular mechanics and the AM1 semiempirical method to study noncovalent interactions. To study the model amidation reaction with methylamine, the two-level ONIOM technique was employed in which the higher level was treated with B3LYP/6-31G(d) DFT, and the lower level was described with either universal force field (UFF) molecular mechanics or AM1. In the single-level calculations, the molecular mechanics strongly overestimated van der Waals interactions of amine molecules with the nanotube walls whereas totally ignored hydrogen bond formation between NH_2 and COOH groups. On the contrary, AM1 calculations produced unrealistic hydrogen-bonded structures where no attraction was manifested between the hydrophobic fragments. In the ONIOM calculations at the B3LYP/6-31G(d):UFF level of theory, CH_3 group of methylamine was strongly attracted to the nanotube, and its N−C bond was directed toward SWNT's center of mass in reaction complex, transition state, and product. Correspondingly, free rotation around C−C(═O)O bond was hampered, which resulted in the existence of two series of isomers, depending on where the methylamine moiety is located, inside or outside the nanotube cavity. At the B3LYP/6-31G(d):AM1 level of theory, attraction between the hydrophobic moieties was very weak or absent, and both "inside" and "outside" starting geometries resulted in very similar reaction complexes, with the N−C bond of methylamine turned outward the nanotube. In addition to that, problems were found in the optimizations requiring force-constant calculations (transition states and vibrational frequencies). In all the ONIOM calculations, the formation of amide derivatives on carboxylated armchair SWNT tips was more energetically preferable than that on the zigzag nanotubes. In addition, in some cases of the "inside" zigzag isomers the reaction was endothermic, whereas it was always exothermic for their armchair models. To study theoretically chemical reactions on carbon nanotube tips by ONIOM technique, where the higher level is treated with B3LYP density functional theory, we recommend UFF molecular mechanics versus the AM1 semiempirical method for the lower-level description. To avoid artifacts associated with wall effects inside the nanotube cavity (such as unrealistically long N−H···O separations, which are supposed to be hydrogen bonds in reaction complexes), the use of nanotube diameters close to the commonly observed SWNT diameters is recommended.

I. Introduction

Among all the existing computational methods to study thermodynamics and mechanisms of chemical reactions, not many of them can be easily applied to carbon nanotubes (CNTs), due to the large size of CNT molecules. Fortunately, a growing need for theoretical approaches capable of treating large (including biochemical) molecular systems gave rise to the development of combined quantum mechanical/molecular mechanical (QM/MM) models, in particular the two or three-level ONIOM method.[1,2] The latter implies dividing a large molecular system into two or three levels. A relatively small section, essential for studying the property of interest, is treated at a higher theoretical level (usually ab initio or DFT). The remaining one or two layers, serving mostly to constrain the general geometry, are described by a computationally less expensive method (molecular mechanics or semiempirical).

The ONIOM approach very soon became an indispensable tool to give insight into chemical structure, reactivity, and spectral properties of CNTs, in particular, single-walled carbon nanotubes (SWNTs). The examples are theoretical studies of the addition of hydrogen and fluorine atoms at zigzag and armchair SWNT side walls,[3−7] using hydrogen and chlorine on Si(111)/SWNT system for data storage,[8] interaction of molecular oxygen with a (9,0) carbon nanotube,[9] organic functionalization of CNT sidewalls by Diels−Alder reactions,[10] sidewall oxidation and complexation by base-catalyzed cycloaddition of transition metal oxide (OsO_4),[11] SWNT sidewall ozonization,[12] structure and Raman spectra for pristine and oxidized carbon nanotube forms,[13] local gating at SWNT walls with photoswitchable biindanylidenes,[14] as well as our papers on the direct amidation[15,16] and esterification[17] of monocarboxy-substituted tips of zigzag and armchair SWNTs with methylamine and methanol, respectively, according to the following reaction schemes:

$$\text{SWNT}-\text{COOH} + \text{H}_2\text{NCH}_3 \rightarrow \text{SWNT}-\text{CO}-\text{NHCH}_3 + \text{H}_2\text{O} \quad (1)$$

$$\text{SWNT}-\text{COOH} + \text{HOCH}_3 \rightarrow \text{SWNT}-\text{CO}-\text{OCH}_3 + \text{H}_2\text{O} \quad (2)$$

* E-mail: basiuk@nuclecu.unam.mx. Fax: (52) 55 56 16 22 33.

10.1021/jp034829m CCC: $25.00
Published on Web 08/06/2003

In addition to the above works, but without treating CNT structures directly, the use of small graphite sheet models along with the ONIOM calculations was suggested as a cost-effective computational strategy for quantum chemistry studies of CNT-related systems.[18]

SWNT models and theoretical levels employed vary to some extent. In most works, the universal force field (UFF)[19] molecular mechanics was used for the lower-level treatment, and the Becke's three-parameter hybrid method[20] with the exchange functional of Lee, Yang, and Parr[21] (B3LYP) was used for the higher-level description,[3−5,7,8,10−17] usually in conjunction with the Pople basis sets. In some cases, AM1 semiempirical description was employed for the lower level.[8,10,12] There is one example of using the second-order Møller−Plesset perturbation theory for the higher-level description (MP2/6-311+G(d,p):UFF and MP2/6-311++G(3df,3pd):UFF),[9] as well as of B3LYP calculations at both levels (B3LYP/6-31G(Od):B3LYP/STO-3G).[13]

The choice of SWNT models depends on what property is to be studied. For example, the nanotube length (of ca. 10−20 Å) is essential to study the addition of hydrogen and fluorine atoms to CNT sidewalls.[3−7] On the other hand, it is of secondary importance in the case of chemical reactions at CNT open ends,[22] so that the models employed may apparently be limited to 2−3 aromatic ring belts only.[15−17] Regarding the SWNT diameter, there is a general trend to use small-diameter nanotube models, in particular, armchair (5,5)[8,10−12,15,16] (diameter of 6.8 Å,[10,12] optimized at the B3LYP/6-31G(d):AM1 level of theory) and zigzag (10,0)[3−5,7,15,16] SWNTs of similar size, to reduce computation cost. Such models can be realistic for a limited number of cases only, because SWNTs more often produced experimentally have diameters of 10−14 Å (1−1.4 nm). Such most typical diameters are matched by only a few models used up to now, zigzag (17,0) (1.33 nm, as calculated at the B3LYP/6-31G(d):UFF theoretical level),[14] (16,0) and armchair (10,10).[17]

Whether the diameter of the nanotube model is important and influences the results of calculations depends on the chemical system studied. In the case of small molecules (H_2, O_2, O_3, H_2O, etc.) or atoms reacting with SWNT tip, its effect can be expected to be insignificant. However, if the reactant species has a bigger size (of a few angstroms), it becomes comparable with the diameter of nanotube cavity. From common considerations, one cannot neglect anymore the proximity of surrounding nanotube walls, which can at least interact with the reactant through van der Waals forces.

An indication that such effects might be important is our recent theoretical results on the direct formation of amides with carboxylic groups on armchair and zigzag SWNT tips, according to reaction 1.[15,16] The models we used were relatively narrow, zigzag (10,0) and armchair (5,5). We found that the methyl amide formation on the armchair SWNT tips is much more energetically preferable than that on the zigzag nanotube tips. At the same time, a detailed inspection of the geometry of hydrogen-bonded reaction complexes revealed that within such narrow cavities, the opposite SWNT wall attracts methylamine molecule, making it equilibrate close to the nanotube axis. In turn, this can dramatically influence the methylamine molecule's position with respect to the carboxylic group, resulting in unrealistically long N−H···O separations supposed to be hydrogen bonds. Apparently, this might produce significant errors in energy estimates for the reaction complexes.

In a later work,[17] we studied a similar reaction of direct esterification of carboxylic groups on armchair and zigzag SWNT tips with methanol (reaction 2). To avoid such undesirable effects as the unrealistically long N−H···O separations, we employed armchair (10,10) and zigzag (16,0) nanotube models. Their calculated diameters are of ca. 1.3−1.4 nm, approaching commonly observed SWNT diameters. Indeed, in this case no anomalous increase of N−H···O separations in the reaction complexes was found, indicating that the diameter of nanotube model is an important factor in such calculations.

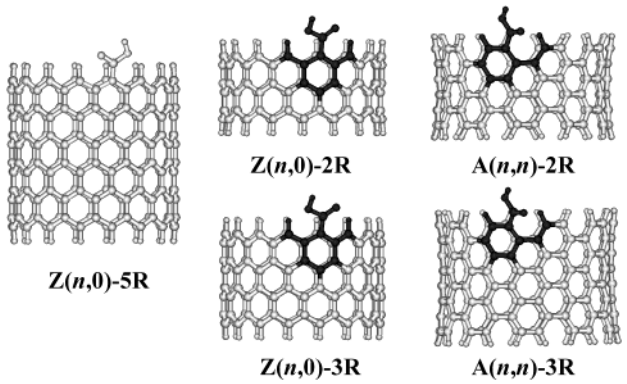

Figure 1. Models of monocarboxy-substituted SWNTs used for MM, QM/MM, and QM/QM calculations. Z = zigzag, A = armchair. Z(*n*,0)-2R, Z(*n*,0)-3R, and Z(*n*,0)-5R are exemplified by the models with $n = 16$; A(*n*,*n*)-2R and A(*n*,*n*)-3R, by the models with $n = 10$. The 2R and 3R models were used for two-level ONIOM calculations; the highlighted (dark) atoms and those belonging to methylamine molecule were treated at the higher (B3LYP) level, and the remaining SWNT atoms were treated with UFF molecular mechanics or the AM1 semiempirical method.

The amidation and esterification reactions are considered especially important for CNT chemistry. The reason is that revealing the energetic preference in the direct formation of amides and esters on armchair SWNT tips versus zigzag nanotube tips might open a new route to selective derivatization of different forms of CNTs, and thus helping their separation and purification due to differences in solubility.[15−17] However, the existence of geometric anomalies can make one suspect that employing more realistic (or typical) nanotube models will alter the calculation results and final conclusions. That is why in the present work we verified them for the amidation reaction 1, by using armchair (10,10) and zigzag (16,0) nanotube models. The highest level of theory used in this work is DFT. Although this theory is known to, in general, be less accurate than many ab initio methods, the size of the systems studied in this work limits us to this approach, and we assume that this theory yields reasonably accurate results for our systems. One more point of interest was whether the AM1 semiempirical method can be used instead of UFF molecular mechanics for the lower-level description in our case, likewise it was done for some other reactions,[8,10,12] and whether it can significantly alter the results. The interaction of aliphatic amines with different monocarboxy-substituted SWNT fragments was additionally tested by single-level AM1 and molecular mechanics calculations.

II. Computational Details

SWNT models and notations used are shown in Figure 1. For the simplest single-level molecular mechanics calculations of interaction of aliphatic amines with monocarboxy-substituted SWNT fragments, we used three (Z(*n*,0)-3R and A(*n*,*n*)-3R) and five (Z(*n*,0)-5R) aromatic ring-belt models of variable diameter. Dangling bonds at the nanotube edges were filled with hydrogen atoms. MM+ force field implemented in HyperChem version 5.1 package (by HyperCube Inc., Canada) was used. Geometry optimization was performed with the Polak-Ribiere

conjugate gradient algorithm and a root-mean-square (RMS) gradient of 0.001 kcal $Å^{-1}$ mol^{-1}. For similar single-level AM1 semiempirical calculations, we used the two and three aromatic ring-belt zigzag models with AM1 method implemented in the Gaussian 98W suite of programs.[23a]

The reactions with methylamine were studied with the nanotube models similar to those described in our previous studies,[15−17] using a two-level ONIOM approach[1,2] implemented in the Gaussian 98W suite of programs. The higher (quantum mechanics) level included the atoms belonging to methylamine molecule and the terminal carboxylic group together with their adjacent C and H atoms (dark atoms in Figure 1). The interaction between the MO and MM regions is treated at the MM level, by using mechanical embedding scheme. Atoms in a lower level bound to an atom in a higher level are replaced by hydrogen atoms during the higher-level part of the ONIOM calculation.[23b] The Becke's three-parameter hybrid method[20] with the exchange functional of Lee, Yang, and Parr[21] (B3LYP) was used for the higher-level description, in conjunction with the 6-31G(d) basis set by Pople et al.[24−26] The remaining nanotube atoms were treated with UFF molecular mechanics[19] (for Z(10,0)-2R, A(5,5)-2R, Z(16,0)-3R, and A(10,10)-3R models) or AM1 semiempirical method (for Z(10,0)-2R, A(5,5)-2R, Z(16,0)-2R, and A(10,10)-2R models).

The stationary point geometries were fully optimized and characterized as minima (0 imaginary frequencies; for reactants, reaction complexes, and products) or first-order saddle points (1 imaginary frequency; for transition states) by vibration frequency calculations. All the optimizations met the default convergence criteria set in Gaussian 98W. We present not only the calculated B3LYP energies (as it was in the previous works), but also extrapolated ONIOM energies as well as the corresponding zero-point energy-corrected (ZPE) values for comparison.

III. Results and Discussion

To estimate qualitatively the lower level contribution, we first performed single-layer MM+ molecular mechanics and AM1 semiempirical modeling of interactions of simple amines with monocarboxy-substituted SWNT fragments with variable diameter and length. A point of particular interest was whether there is a well-manifested energetic difference between adsorption outside and inside the nanotube cavity:[15] in the latter case, one can expect stronger interaction due to a cooperative wall effect, that is, a phenomenon similar to capillary condensation in narrow pores. From common considerations, the smaller the SWNT diameter, the bigger this difference should be. At the same time, there must be a lower SWNT diameter limit, where amine molecule does not fit the cavity anymore. On the other hand, increasing the nanotube diameter should result in decreasing the energy difference.

For MM+ modeling, we used monocarboxy-substituted Z(*n*,0)-3R, A(*n*,*n*)-3R, and Z(*n*,0)-5R nanotube models, whereas ammonia, methylamine, *n*-propylamine, and *n*-nonylamine were tested as adsorbates. The nanotube length was sufficient to accommodate one alkylamine (or ammonia) molecule, oriented in parallel. A conformation and exact position of amine molecule (especially for *n*-propylamine and *n*-nonylamine) with respect to the nanotube model can noticeably influence the calculated value of interaction energy. Therefore, to obtain comparable results, in all simulations we used the same starting geometry, where the following three criteria were met: (i) the amino group was placed close to the SWNT carboxylic group, (ii) the two molecules were parallel to each other (for the case of alkylamines), and (iii) the carbon chain plane (for the case of *n*-propylamine and *n*-nonylamine) was parallel to the closest SWNT wall.

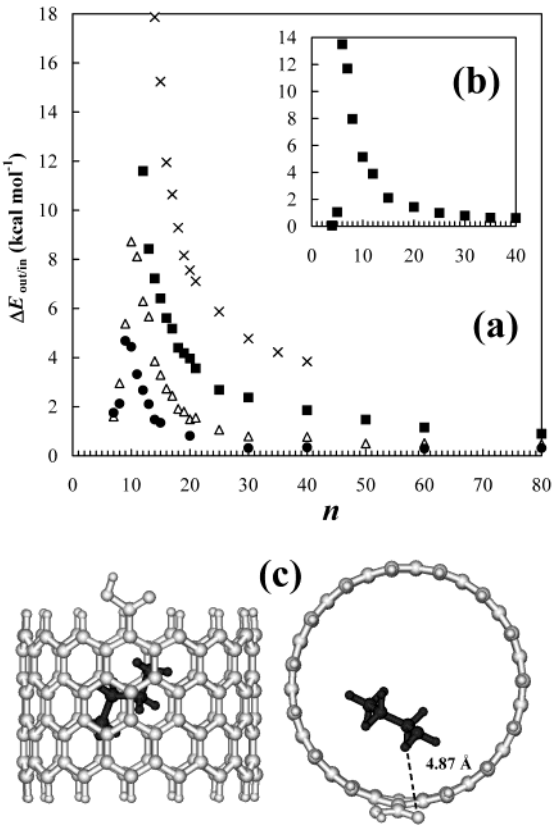

Figure 2. Effect of nanotube diameter (expressed as *n*) on the difference between total energies of amine interaction with the outside and inside walls ($\Delta E_{out/in} = E_{out} - E_{in}$) of monocarboxy-substituted SWNTs, as calculated by MM+ molecular mechanics: (a) NH_3 (●), CH_3NH_2 (△), $CH_3(CH_2)_2NH_2$ (■) with Z(*n*,0)-3R SWNTs, and $CH_3(CH_2)_8NH_2$ (×) with Z(*n*,0)-5R; (b) $CH_3(CH_2)_2NH_2$ (■) with A(*n*,*n*)-3R. (c) Position of $CH_3(CH_2)_2NH_2$ molecule (dark) inside Z(15,0)-3R SWNT-COOH; the shortest distances between them (CH···C_{wall}) are less than 3 Å, whereas NH···O separation is almost 5 Å.

The results are presented in Figure 2 as plots of the energetic difference $\Delta E_{out/in} = E_{out} - E_{in}$ (in kcal mol^{-1}) versus the *n* value in Z(*n*,0) and A(*n*,*n*) nanotubes. For narrower zigzag SWNTs ($n = 7-13$), which are more strained due to a stronger distortion from the plain graphite sheet, the calculated total energies had positive values; they became negative starting with (14,0) SWNT. For the armchair models, the MM+ energies were positive for $n = 4$ to 9, and negative starting with $n = 10$. Ammonia molecule fits inside the nanotube starting with $n = 9$; here the energy difference $\Delta E_{out/in}$ has the highest value, then it rapidly decreases and does not show notable changes after $n = 20$ (Figure 2a). Methylamine has a slightly bigger molecule size, fitting inside Z(10,0) (highest $\Delta E_{out/in}$ value) and wider SWNTs; similarly to NH_3, the energy difference does not show significant changes after ca. $n = 20$.

Bigger nanotube diameters are required to accommodate longer-chain amines (*n*-propylamine and *n*-nonylamine) inside the cavity, Z(12,0) and A(6,6) (the highest $\Delta E_{out/in}$ value in Figure 2b). The biggest energetic difference (of ca. 28 kcal mol^{-1}; outside the plot area shown in Figure 2a) between adsorption outside and inside SWNT, was obtained for nonylamine at Z(12,0)-5R SWNT; then, similarly to other amines and ammonia, $\Delta E_{out/in}$ drops rapidly with increasing *n* up to approximately 20, and its further decrease becomes very slow: even for Z(30,0)-5R nanotube (whose diameter is 2.3 nm for

the MM+ geometry), $\Delta E_{out/in}$ is almost 5 kcal mol^{-1}. Thus, the energetic difference $\Delta E_{out/in}$ should be significant for a wide size range of CNTs (both single- and multiwalled) and the preferential sites for adsorption of long-chain amines (and most likely of other organic molecules) are inside SWNTs.

For all three alkylamines in narrower SWNTs, in the optimized "inside" complexes the molecules tended to remain parallel. When increased SWNT diameter, the amine gradually inclined with respect to the nanotube axis, as it is shown for $CH_3(CH_2)_2NH_2$ molecule inside monocarboxy Z(15,0)-3R in Figure 2c. In the "outside" complexes, this effect was observed for even narrower SWNTs. For example, for Z(12,0)-5R and nonylamine, the angle between SWNT and nonylamine axes was about 10°. For Z(30,0)-5R, this angle in both "inside" and "outside" complex reached as much as 30° and for even higher *n* values (e.g., 40 and 60), the rotation increases further (we have not been able to finish the geometry optimization due to convergence problems). This trend was even more striking for methylamine interacting with Z(*n*,0)-3R nanotube models, where due to an easier convergence we optimized the complexes for *n* values up to 80: the angle between the nanotube axis and the C−N bond was close to 60° with the amino group turned to a random direction with respect to the position of COOH group.

The above observations lead to a conclusion that van der Waals interactions make a major contribution into amine adsorption on carboxy-substituted SWNTs, as modeled by MM+ molecular mechanics, whereas the interaction between the polar NH_2 and COOH groups does not manifest at all. As can be seen in Figure 2c, showing the position of $CH_3(CH_2)_2$-NH_2 molecule inside a relatively narrow monocarboxylated Z(15,0)-3R, the NH···O separation is almost 5 Å, which by no means can be qualified as hydrogen bond (for comparison, the shortest distance between the molecules CH···C_{wall} is less than 3 Å).

Semiempirical calculations with AM1 method produced totally different results. Since AM1 is much more computationally demanding than molecular mechanics, the nanotube models (all zigzag) themselves were reduced to two or at best three belts of aromatic rings, with a maximum *n* value of 15 (Figures 3 and 4). A preliminary test with simplified models including a butane molecule and non-carboxylated Z(*n*,0) SWNTs showed that the butane molecule barely enters into the cavity at $n = 15$, being centered at the nanotube axis (Figure 3; compare to Figure 2c). Consequently, the interaction with SWNT walls is very weak. A similar result was obtained with butane molecule positioned outside the nanotube cavity. Thus, it was not surprising to find no substantial energetic differences for the adsorption inside and outside model SWNTs.

The pattern of amine interaction with carboxylated nanotube fragments completely changes as well, as compared to the MM+ results. It can be best exemplified for nonylamine and monocarboxy-substituted Z(16,0)-3R SWNT (Figure 4). Amino group of nonylamine molecule placed inside the nanotube, is strongly attracted to the carboxylic group, forming a hydrogen bond with NH···O═C separation of 2.42 Å (Figure 4a). As was mentioned in the previous paragraph, a Z(15,0) SWNT cavity can barely adopt a small hydrocarbon molecule. In the case of nonylamine, its H-bond interaction with the COOH group makes the nonyl radical deviate from the coaxial position and adopt a slightly bent conformation. This bending does not happen if nonylamine molecule was initially placed outside the nanotube cavity. The molecule remains aligned, forming hydrogen bond between the NH_2 and COOH groups, and showing no sign of interaction between the hydrophobic nonyl radical and SWNT wall (Figure 4b). Both H atoms of the amino group participate in hydrogen bonding with the carbonyl group, with slightly different NH··· O═C separations, of 2.39 and 2.54 Å. We tried to change the initial position of nonylamine with respect to the COOH group, and found that H-bonding with the OH group instead of C═O is possible as well. However the general feature, that is no manifestation of interaction between the hydrophobic nonyl radical and SWNT wall, did not change. Thus, contrary to MM+ molecular mechanics, the AM1 semiempirical method accounts well for hydrogen bonding between the NH_2 and COOH groups, but completely neglects interaction between the hydrophobic fragments.

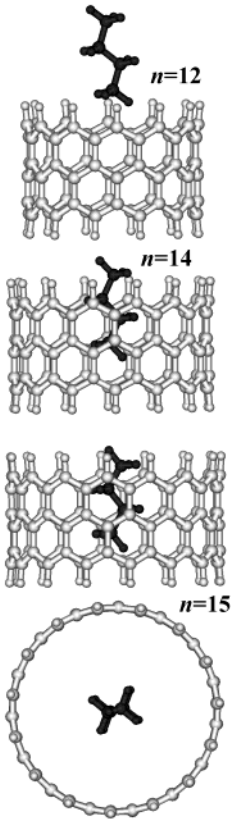

Figure 3. AM1 semiempirical estimates of the narrowest cavity capable to accommodate a linear hydrocarbon, exemplified by Z(*n*,0)-2R SWNTs and butane, respectively. Butane molecule (dark) enters completely only starting with $n = 15$, and does not approach the nanotube walls closer than 4.4 Å.

On the basis of the above observations only, it is difficult to give a preference to molecular mechanics or AM1 quantum mechanics for the lower-level description in ONIOM calculations. An important factor is cost-efficiency, and from this point of view the use of molecular mechanics seems more attractive. We performed a series of ONIOM calculations for the amidation reaction 1 similar to those reported earlier[15,16] using UFF molecular mechanics and the AM1 semiempirical method for the lower level. The higher level was treated at the B3LYP/6-31G(d) level of theory in all cases. In the chemical models employed the high level included the atoms belonging to methylamine molecule and the terminal carboxylic group, together with their adjacent C and H atoms (dark atoms in Figure 1). The remaining part of the nanotube was variable in diameter and length. For B3LYP/6-31G(d):UFF calculations, we tested narrow and short SWNTs Z(10,0)-2R and A(5,5)-2R,[15,16] as well as wider and longer models Z(16,0)-3R and A(10,10)-3R.[17] For B3LYP/6-31G(d):AM1 calculations, the use of wider models with three complete belts of aromatic rings was not possible due to limited computational resources, and short SWNT models

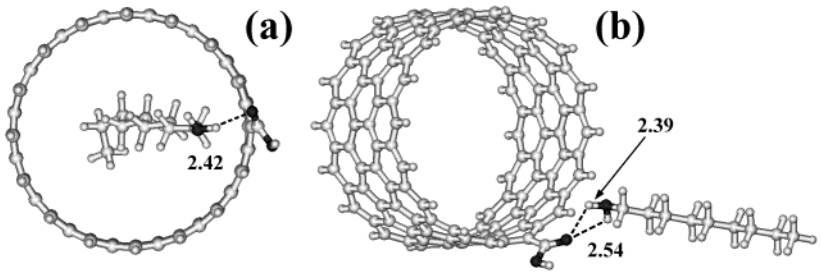

Figure 4. Hydrogen bonded complexes of $CH_3(CH_2)_8NH_2$ with carboxylic group of Z(16,0)-3R SWNT-COOH, optimized by the AM1 semiempirical method. In the input structures, nonylamine molecule was placed inside (a) and outside the nanotube cavity (b). Interatomic distances in angstroms. H-bonding with the OH group instead of carbonyl is possible as well.

TABLE 1: Energies Relative to Reactant Level for Reaction Complexes (RC), Transition States (TS), Hydrogen-Bonded Products (P), and Separated Products (P(sep)) for the Gas-Phase Amidation Reaction of Monocarboxy-Substituted SWNTs with Methylamine, Calculated for Different SWNT Models (Figure 1) at Different Theoretical Levels[a]

	relative energy (kcal mol^{-1}): B3LYP/ONIOM/ZPE-ONIOM			
theoretical level/model	RC_{in} [RC_{out}]	TS_{in} [TS_{out}]	P_{in} [P_{out}]	P_{in}(sep) [P_{out}(sep)]
B3LYP/6-31G(d):UFF				
Z(10,0)-2R[b]	−2.6/−18.0/−17.3	48.8/44.8/46.7	−1.5/−5.8/−5.6	12.8/8.5/5.9
	[*c*]	[*c*]	[*c*]	[*c*]
A(5,5)-2R[b]	−2.9/−8.1/−7.0	51.1/35.9/32.1	−9.0/−10.3/−9.6	4.7/3.4/1.4
	[*c*]	[*c*]	[*c*]	[*c*]
B3LYP/6-31G(d):AM1				
Z(10,0)-2R	−12.2/−14.6/−13.0	52.3/47.4/46.1	0.8/−5.8/−5.0	15.1/8.2/6.2
	[−12.1/−14.6/*d*]	[*d*]	[−3.2/−8.8/−7.5]	[10.7/4.5/*d*]
A(5,5)-2R	−4.8/−5.6/−4.7	54.4/50.4/48.9	−8.3/−6.9/−6.1	5.4/6.6/4.8
	[*c*]	[*c*]	[*c*]	[*c*]
B3LYP/6-31G(d):AM1				
Z(16,0)-2R	−12.2/−14.6/*d*	*c*	−0.6/−8.0/*d*	13.6/5.9/*d*
	[*c*]	[*c*]	[*c*]	[*c*]
A(10,10)-2R	−6.0/−6.1/*d*	*c*	−11.1/−10.2/*d*	2.4/3.2/*d*
	[*c*]	[*c*]	[*c*]	[*c*]
B3LYP/6-31G(d):UFF				
Z(16,0)-3R	−2.4/−4.3/−3.5	51.4/52.0/50.1	1.4/1.2/1.6	15.7/15.5/13.1
	[−5.1/−10.2/−9.9]	[47.4/45.8/45.3]	[−4.9/−5.3/−4.5]	[9.0/8.4/6.6]
A(10,10)-3R	−1.9/−11.2/−11.4	38.3/24.5/22.3	−14.0/−25.6/−26.0	−0.3/−11.8/−15.0
	[−10.3/−22.3/−22.8]	[41.0/27.9/25.3]	[−12.5/−23.9/−24.3]	−0.8/−14.9/−18.5

[a] B3LYP, ONIOM, and zero-point energy-corrected (ZPE) ONIOM energies are specified. RC_{in}, TS_{in}, P_{in}, and P_{in}(sep) correspond to orientation of methylamine inward the nanotube cavity; RC_{out}, TS_{out}, P_{out} and P_{out}(sep), outward the nanotube cavity. [b] Ref 16. [c] Not calculated. [d] Calculations failed.

were considered only, that is Z(10,0)-2R, A(5,5)-2R, Z(16,0)-2R, and A(10,10)-2R.

Table 1 includes calculated energies (relative to the level of separated reactants) for reaction complexes (RC), transition states (TS), hydrogen-bonded products (P) as well as sums of energies of separated products (amidated nanotube and water molecule; P(sep)). The energies presented are B3LYP, ONIOM, and zero-point energy-corrected ONIOM energies (ZPE-ONIOM). As in the single-level MM+ and AM1 calculations, we tested different orientations of methylamine with respect to the nanotube. RC_{in}, TS_{in}, P_{in}, and P_{in}(sep) correspond to the orientation of methylamine inward the nanotube cavity; RC_{out}, TS_{out}, P_{out}, and P_{out}(sep), outward the nanotube cavity. The resulting optimized geometries are exemplified for Z(16,0)-3R (Figure 5) and A(10,10)-3R models (Figure 6), as computed at the B3LYP/6-31G(d):UFF level of theory. However, with AM1 lower-level description, not all the calculations can be successfully performed: while the optimization itself was completed smoothly (and B3LYP and ONIOM energies were retrieved; Table 1), force-constant and frequency calculations usually failed due to self-consistence problems. This circumstance prohibited transition state optimizations, which often require force-constant calculation at every step.

The choice of lower-level description influences mutual orientation of the amine and nanotube components as well. A general trend here is similar to the one found in the single-level calculations. At the B3LYP/6-31G(d):UFF level of theory, CH_3 group of methylamine is strongly attracted to the nanotube, and its N−C bond is turned toward SWNT's center of mass. At the B3LYP/6-31G(d):AM1 level of theory, their mutual orientation reminds the one shown in Figure 4b: since attraction between the hydrophobic moieties is very weak (if any), both "inside" and "outside" starting geometries produce very similar reaction complexes, with N−C bond turned outward the nanotube. Correspondingly, their energies differ insignificantly, by less than 0.1 kcal mol^{-1} (Table 1, for Z(10,0)-2R). In the amide products, the freedom of methylamine moiety is restricted, and the "inside" and "outside" isomers are distinct, as expected, in terms of both geometry and energy.

As regards the selectivity of amidation reaction 1 at carboxylated tips of zigzag and armchair nanotubes,[15,16] this conclusion remains valid at the B3LYP/6-31G(d):AM1 theoretical level. Taking into consideration all the energies calculated (B3LYP, ONIOM and ZPE-ONIOM; Table 1), in both series of calculations (Z(10,0)-2R versus A(5,5)-2R, and Z(16,0)-2R versus A(10,10)-2R), amidation of the armchair SWNT tips is more preferable than in the case of their zigzag counterparts. This preference is especially clearly seen for the B3LYP energies, where the difference is ca. 10 kcal mol^{-1}. In addition, reaction complexes are much more stable for the zigzag than for armchair

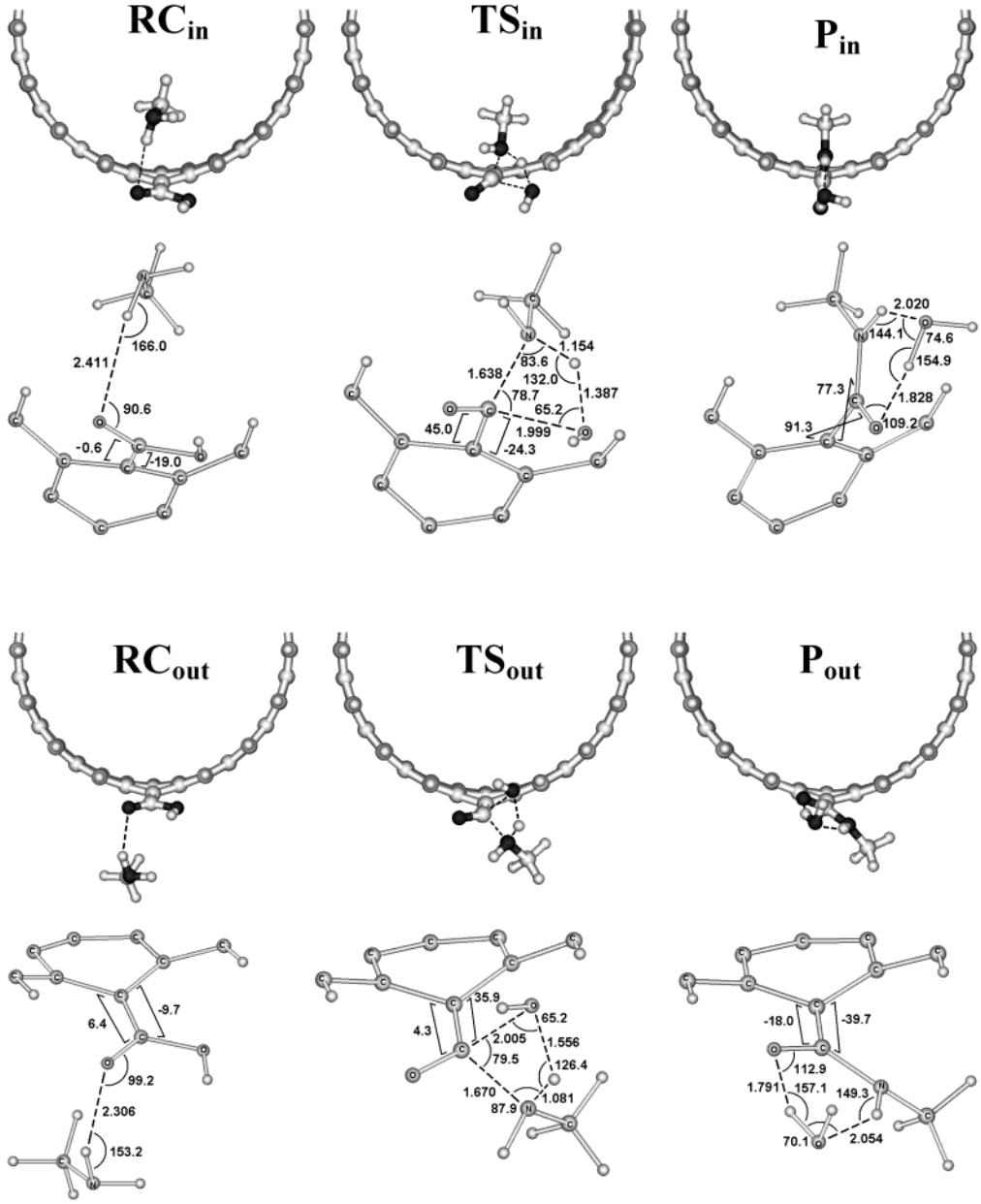

Figure 5. Views along SWNT axis of the reaction complexes (RC), transition states (TS), and products (P) for the gas-phase amidation reaction of monocarboxy-substituted Z(16,0)-3R model SWNT with methylamine, and the fragments treated at the B3LYP/6-31G(d) theoretical level with selected geometric parameters (interatomic distances in Å, bond angles and dihedrals in degrees). In the upper series (RC_{in}, TS_{in}, and P_{in}), methylamine was placed inside the nanotube cavity; in the lower series (RC_{out}, TS_{out}, and P_{out}), outside the nanotube cavity.

nanotubes, by >6 kcal mol^{-1} (any values: B3LYP, ONIOM, and ZPE-ONIOM). Furthermore, their energies turn to be much lower with respect to the corresponding products: this fact makes amidation of the carboxylated zigzag SWNT tips a prohibited reaction at all.[27]

Due to the deficiencies in the results of B3LYP/6-31G(d):AM1 ONIOM calculations for our systems, we further focus on molecular mechanics description of the lower level. As was mentioned in the introduction, a detailed inspection of the geometry of hydrogen-bonded reaction complexes, revealed that within narrow carboxylated SWNTs, surrounding SWNT walls attract methylamine molecule, making it equilibrate close to the nanotube axis. In principle, this might dramatically influence its position with respect to COOH group, resulting in unrealistically long N−H···O separations, which are supposed to be hydrogen bonds, and apparently producing significant errors in energy estimates for RCs. In particular, such long separations were observed for Z(10,0)-2R model, when calculated at the B3LYP/4-31G:UFF and B3LYP/6-31G(d):UFF theoretical levels.[15,16] As can be seen from Figure 5, increasing the nanotube diameter to $n = 16$ (calculated diameter of ca. 1.25 nm approaching realistic, commonly observed SWNT diameters) fixes this problem: in Z-RC_{in} and Z-RC_{out}, the values of N−H··· O separation are quite reasonable, of 2.411 and 2.306 Å, respectively. A similar positive result was obtained with the same SWNT model for esterification reaction 2.[17]

The conclusion on the selectivity of amidation reaction remains valid at the present level of theory for bigger SWNT models. Regardless of the energy values considered (B3LYP, ONIOM, and ZPE-ONIOM; Table 1), in case of the "inside" isomers (upper structures in Figures 5 and 6) the reaction on carboxylated A(10,10)-3R nanotube is exothermic, and endothermic for its zigzag counterpart. The difference in energies of the products exceeds 10 kcal mol^{-1} for B3LYP energies to

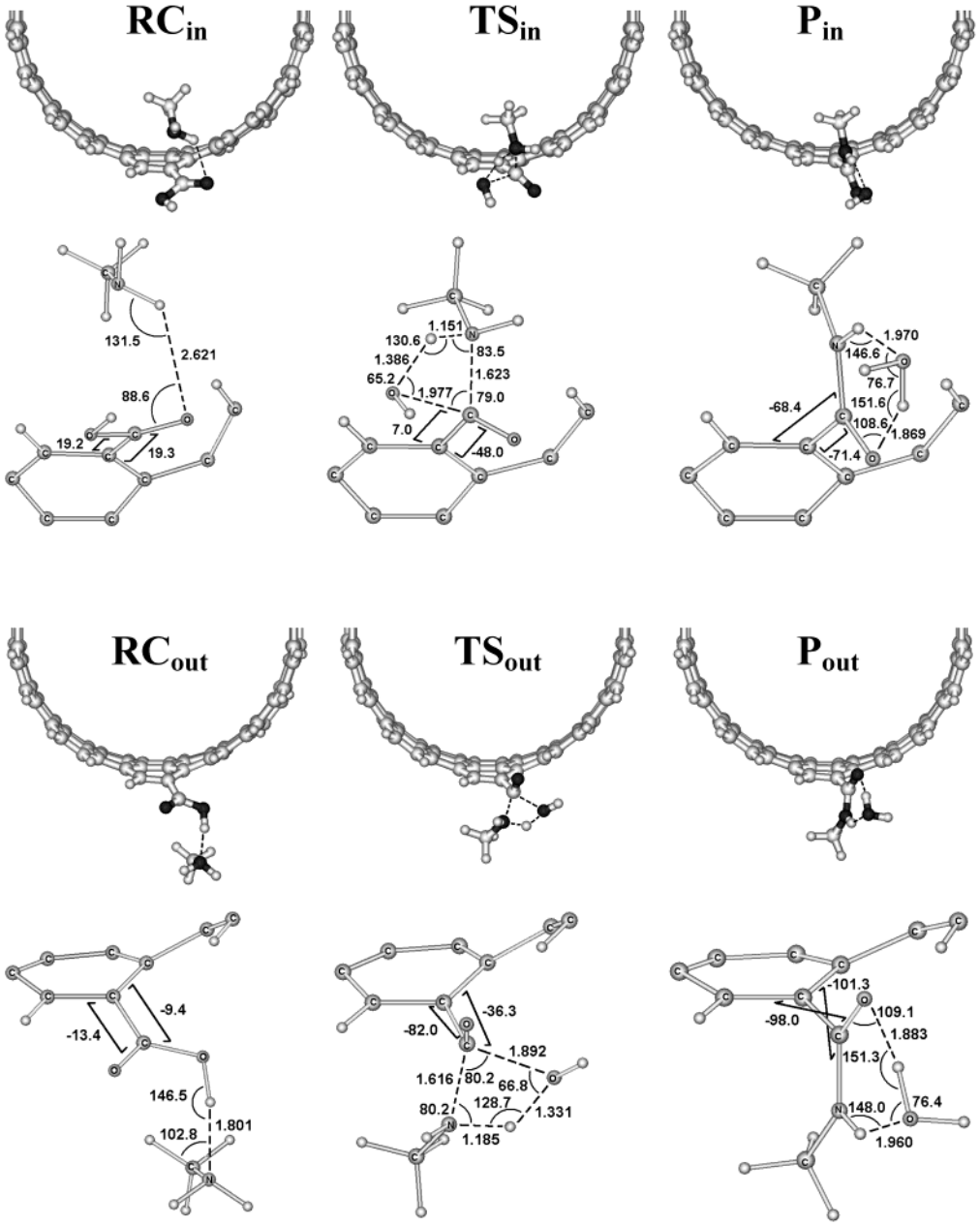

Figure 6. Views along SWNT axis of the reaction complexes (RC), transition states (TS), and products (P) for the gas-phase amidation reaction of monocarboxy-substituted A(10,10)-3R model SWNT with methylamine, and the fragments treated at the B3LYP/6-31G(d) theoretical level with selected geometric parameters (interatomic distances in Å, bond angles and dihedrals in degrees). In the upper series (RC_{in}, TS_{in}, and P_{in}), methylamine was placed inside the nanotube cavity; in the lower series (RC_{out}, TS_{out}, and P_{out}), outside the nanotube cavity.

more than 25 kcal mol^{-1} for ONIOM and ZPE-ONIOM energies. The transition state energies are much lower for the armchair nanotube as well, by ca. 13 kcal mol^{-1} (B3LYP values) to 28 kcal mol^{-1} (ONIOM and ZPE-ONIOM energies). The armchair reaction complex has a slightly higher B3LYP energy than the zigzag reaction complex has (−1.9 vs. −2.4 kcal mol^{-1}), but lays by ca. 7 kcal mol^{-1} lower according to ONIOM and ZPE-ONIOM energy values. The latter observation, however, does not affect the reaction selectivity.

Contrary to the results of B3LYP/6-31G(d):AM1 ONIOM calculations, there are big differences in the geometric and energetic parameters for the "inside" and "outside" isomers computed at the B3LYP/6-31G(d):UFF level of theory. N−C bonds in all the reaction complexes, transition states and products are always directed toward the nanotube, hampering in this way free rotation around C−C(═O)O bond and consequently interconversion of the isomers. This account for van der Waals interactions between the nanotube walls and methyl radical is a substantial argument for the use of UFF molecular mechanics for the lower-level description. It turns out that most energy values calculated for the "outside" RCs, TSs and Ps are lower than the respective energies for the "inside" species, to a different extent; the exceptions are energies for transition state and hydrogen-bonded products in the case of A(10,10)-3R model. But even accounting for this fact, the reaction selectivity remains the same. Although it changes to exothermic for the zigzag nanotube, exothermicity for the armchair model is higher by ca. 8 kcal mol^{-1} (B3LYP energy) to more than 20 kcal mol^{-1} (ONIOM and ZPE-ONIOM energies). The transition state energies are lower for the armchair nanotube as well, by ca. 6 kcal mol^{-1} (B3LYP values) to 20 kcal mol^{-1} (ZPE-ONIOM energy).

The dependence of reaction parameters on mutual spatial orientation of the nanotube and the second reactant, as well as

on CNT diameter, is natural and logic, especially if the second reactant contains a hydrophobic fragment. Thus, it is inferred necessary that the chemical model selected for theoretical description accounts for such steric factors, by having tubular shape and realistic diameter. On the contrary, bidimensional graphite sheet models (like those proposed in ref 18) ignore the effect of nanotube walls and their curvature, and should not be used.

IV. Conclusions

(i) Single-level calculations of aliphatic amine interaction with carboxylated SWNT models, employing MM+ molecular mechanics and the AM1 semiempirical method, produced qualitatively distinct results. The molecular mechanics strongly overestimated van der Waals interactions of amine (and even ammonia) molecules with the nanotube walls, whereas totally ignored hydrogen bond formation between NH_2 (or NH_3) and COOH groups. On the other hand, AM1 calculations produced unrealistic hydrogen-bonded structures where no attraction was manifested between the hydrophobic fragments, even in the case of long-chain aliphatic amines.

(ii) A general trend in the results of ONIOM calculations for the model amidation reaction 1 was similar to the one described in the previous paragraph. At the B3LYP/6-31G(d):UFF level of theory, CH_3 group of methylamine was strongly attracted to the nanotube, and its N−C bond was directed toward SWNT's center of mass in all reaction complexes, transition states and products. Correspondingly, free rotation around C−C(═O)O bond and consequently interconversion of the "inside" and "outside" isomers was hampered. At the B3LYP/6-31G(d):AM1 level of theory, attraction between the hydrophobic moieties was very weak or absent, and both "inside" and "outside" starting geometries resulted in very similar reaction complexes, with the N−C bond of methylamine turned outward the nanotube.

(iii) With both ONIOM techniques tested, our conclusion reported previously[15,16] on the preferable formation of amide derivatives (reaction 1) on the carboxylated armchair SWNT tips versus the zigzag nanotubes remained valid. Furthermore, in some cases of the "inside" zigzag isomers the reaction turned out to be endothermic (this was also the case in single-level AM1 calculations[27]), whereas it was always exothermic for their armchair analogues.

(iv) With the AM1 lower-level description, not all ONIOM calculations were possible to finish. While simple optimization procedures were completed smoothly (B3LYP and ONIOM energies were retrieved), force-constant and frequency calculations usually failed due to self-consistence problems. This prohibited transition state optimizations, which often require force-constant calculation at every step. Thus, the use of AM1 for the lower-level description has serious limitations, at least to study our reaction systems by means of the ONIOM implementation in Gaussian 98W.

(v) While the use of relatively narrow SWNT models (such as Z(10,0) and A(5,5)) in the B3LYP/6-31G(d):UFF ONIOM calculations was noticed to result in unrealistically long N−H···O separations (which are supposed to be hydrogen bonds in reaction complexes), increasing the nanotube diameter to Z(16,0) and A(10,10) (calculated diameters of ca. 1.3−1.4 nm approaching commonly observed SWNT diameters) eliminated this problem.

(vi) To study theoretically chemical reactions on carbon nanotube tips with ONIOM technique, where the higher level is treated with B3LYP density functional theory, we recommend UFF molecular mechanics versus the AM1 semiempirical method for the lower-level description.

Acknowledgment. Financial support from the National Council of Science and Technology of Mexico (Grants CONACYT-36317-E and -40399-Y) and from the National Autonomous University of Mexico (Grants DGAPA-IN100402-3 and -IN102900) is greatly appreciated.

References and Notes

(1) Svensson, M.; Humbel, S.; Froese, R. D. J.; Matsubara, T.; Sieber, S.; Morokuma, K. *J. Phys. Chem.* **1996**, *100*, 19357.

(2) Dapprich, S.; Komáromi, I.; Byun, K. S.; Morokuma, K.; Frisch, M. J. *J. Mol. Struct.: THEOCHEM* **1999**, *461*−*462*, 1.

(3) Bauschlicher, C. W. *Chem. Phys. Lett.* **2000**, *322*, 237.

(4) Bauschlicher, C. W. *Nano Lett.* **2001**, *1*, 223.

(5) Bauschlicher, C. W.; So, C. R. *Nano Lett.* **2002**, *2*, 337.

(6) Froudakis, G. E. *J. Phys.: Condens. Matter* **2002**, *14*, 453.

(7) Froudakis, G. E. *Nano Lett.* **2001**, *1*, 179.

(8) Rosi, M.; Bauschlicher, C. W. *Chem. Phys. Lett.* **2001**, *347*, 291.

(9) Ricca, A.; Drocco, J. A. *Chem. Phys. Lett.* **2002**, *362*, 217.

(10) Lu, X.; Tian, F.; Wang, N.; Zhang, Q. *Org. Lett.* **2002**, *4*, 4313.

(11) Lu, X.; Tian, F.; Feng, Y.; Xu, X.; Wang, N.; Zhang, Q. *Nano Lett.* **2002**, *2*, 1325.

(12) Lu, X.; Zhang, L.; Xu, X.; Wang, N.; Zhang, Q. *J. Phys. Chem. B* **2002**, *106*, 2136.

(13) Irle, S.; Mews, A.; Morokuma, K. *J. Phys. Chem. A* **2002**, *106*, 11973.

(14) Rotkin, S. V.; Zharov, I. *Int. J. Nanosci.* **2002**, *1*, 1.

(15) Basiuk, E. V.; Basiuk, V. A.; Bañuelos, J.-G.; Saniger-Blesa, J.-M.; Pokrovskiy, V. A.; Gromovoy, T. Yu.; Mischanchuk, A. V.; Mischanchuk, B. G. *J. Phys. Chem. B* **2002**, *106*, 1588.

(16) Basiuk, V. A.; Basiuk, E. V.; Saniger-Blesa, J.-M. *Nano Lett.* **2001**, *1*, 657.

(17) Basiuk, V. A. *Nano Lett.* **2002**, *2*, 835.

(18) Montoya, A.; Mondragón, F.; Truong, T. N. *Carbon* **2002**, *40*, 1863.

(19) Rappe, A. K.; Casewit, C. J.; Colwell, K. S.; Goddard, W. A.; Skiff, W. M. *J. Am. Chem. Soc.* **1992**, *114*, 10024.

(20) Becke, A. D. *J. Phys. Chem.* **1993**, *98*, 5648.

(21) Lee, C.; Yang, W.; Parr, R. G. *Phys. Rev. B* **1988**, *37*, 785.

(22) Basiuk, V. A.; Basiuk (Golovataya-Dzhymbeeva), E. V. Chemical Derivatization of Carbon Nanotube Tips. In *Encyclopedia of Nanoscience and Nanotechnology*; Nalwa, H. S., Ed.; American Scientific Publishers: Stevenson Ranch CA, 2003; in press.

(23) (a) Frisch, M. J.; Trucks, G. W.; Schlegel, H. B.; Scuseria, G. E.; Robb, M. A.; Cheeseman, J. R.; Zakrzewski, V. G.; Montgomery, J. A., Jr.; Stratmann, R. E.; Burant, J. C.; Dapprich, S.; Millam, J. M.; Daniels, A. D.; Kudin, K. N.; Strain, M. C.; Farkas, O.; Tomasi, J.; Barone, V.; Cossi, M.; Cammi, R.; Mennucci, B.; Pomelli, C.; Adamo, C.; Clifford, S.; Ochterski, J.; Petersson, G. A.; Ayala, P. Y.; Cui, Q.; Morokuma, K.; Malick, D. K.; Rabuck, A. D.; Raghavachari, K.; Foresman, J. B.; Cioslowski, J.; Ortiz, J. V.; Baboul, A. G.; Stefanov, B. B.; Liu, G.; Liashenko, A.; Piskorz, P.; Komaromi, I.; Gomperts, R.; Martin, R. L.; Fox, D. J.; Keith, T.; Al-Laham, M. A.; Peng, C. Y.; Nanayakkara, A.; Challacombe, M.; Gill, P. M. W.; Johnson, B. G.; Chen, W.; Wong, M. W.; Andres, J. L.; Gonzalez, C.; Head-Gordon, M.; Replogle, E. S.; Pople, J. A. *Gaussian 98W*, revision A.9; Gaussian, Inc.: Pittsburgh, PA, 1998. (b) Frisch, Æ; Frisch, M. J. *Gaussian 98 User's Reference*, 2nd ed.; Gaussian, Inc.: Pittsburgh, PA, 1999.

(24) Hariharan, P. C.; Pople, J. A. *Chem. Phys. Lett.* **1972**, *66*, 217.

(25) Binkley, J. S.; Pople, J. A. *Int. J. Quantum Chem.* **1975**, *9*, 229.

(26) Krishnan, R.; Frisch, M. J.; Pople, J. A. *J. Chem. Phys.* **1980**, *72*, 4244.

(27) We also performed single-layer AM1 calculations for the amidation of monocarboxy Z(16,0)-3R and A(10,10)-3R SWNTs with methylamine to form products P_{in} similar to those shown in Figures 5 and 6, respectively. The reaction for the armchair species was found to be 0.6 kcal mol^{-1} exothermic, whereas for the zigzag species it was 2.9 kcal mol^{-1} endothermic, and thus unfavorable like at all other theoretical levels. The most notable difference in P_{in} geometries obtained with AM1 as compared to those from the ONIOM calculations, is that the H_2O molecule forms hydrogen bonds with the carbonyl group only, and not with the NH group.